Journal of Applied Research and Technology

www.jart.icat.unam.mx

Journal of Applied Research and Technology 19 (2021) 521-539

Original

Production and characterization of activated carbon from pineapple stubble for removal of methylene blue and surfactants

D. Montenegro[a]* • N. Montero[a] • R. A. Hernández[b] • J. Méndez[c]

[a]*University of Costa Rica, School of Chemical Engineering, San José, Costa Rica*
[b]*State Distance University, Bioenergetic and Environmental Research Unit, San José, Costa Rica*
[c]*University of Costa Rica, Forest Resources Unit, Engineering Research Institute, San José, Costa Rica*

Received 02 24 2021; accepted 05 09 2021
Available 10 31 2021

Abstract: The objective of this work was to produce activated carbon from the agricultural waste known as pineapple stubble and to test its effectiveness in the removal of methylene blue and surfactants. Activated carbon was prepared using $ZnCl_2$ and H_3PO_4 as activating agents and impregnation ratios of 2: 1 and 4:1 between the agent (mL) and the precursor (g) were evaluated. It was also investigated the need or not of a drying stage prior to carbonization. The produced activated carbon was characterized through FT-IR spectroscopy, X-ray fluorescence, N_2 physisorption analysis, elemental analysis, and electron microscopy. Methylene blue adsorption tests were performed to determine the adsorption effectiveness of the different activated carbons produced. For such evaluation, a 2^3 factorial design was used, and statistical analysis determined that the activated carbon with the highest adsorption of methylene is produced under the following conditions: $ZnCl_2$ as an activating agent, an impregnation ratio of 4:1, and with no drying step prior to carbonization. This produced activated carbon is also effective in the adsorption of the surfactant sodium dodecyl sulfate and for the surfactants present in the gray water obtained after washing clothes with commercial detergent. In these cases, removal efficiencies above 98 % were achieved. Concerning the characteristics of this activated carbon, it was observed a surface area of 685.5 m^2/g, a total pore volume of 0.53 cm^3/g, and an average pore diameter of 3.1 nm. Results achieved in the present study demonstrate that is possible to produce effective activated carbon for the removal of methylene blue and surfactants from agricultural waste such as pineapple stubble.

Keywords: pineapple stubble, activated carbon, surfactant, methylene blue, zinc chloride

*Corresponding author.
E-mail address: dmontenegroq96@gmail.com(D. Montenegro).
Peer Review under the responsibility of Universidad Nacional Autónoma de México.

1. Introduction

In Costa Rica, pineapple cultivation is well-established and developed. In 2019, 2.1 million tons were exported, which generated US $ 962 million concerning the exportation of fresh fruits, making Costa Rica the largest exporter of fresh pineapple in the world (Ministerio Comercio Exterior de Costa Rica, 2020). The National Chamber of Pineapple Producers and Exporters (CANAPEP) reports 170 producers, providing about 28,000 direct jobs and 105,000 indirect jobs. It is estimated that pineapple cultivation covers an area of 40,000 hectares (CANAPEP, 2020). Other studies indicate that the crop cover is higher than 65,000 ha. Such difference is because it is not mandatory to be linked or registered in CANAPEP.

Once the fruit is harvested, and the useful cycle of the plant ends, a residue called stubble remains in the field, which corresponds to the stems, leaves, and roots of the pineapple plant which currently have no commercial value. Based on the report of cultivated hectares and applying the empirical relationship developed by Hernández-Chaverri and Prado-Barragán (2018), it is estimated that approximately (3,983 ± 1,192) million tons are produced per year on a wet basis of stubble (Hernández-Chaverri & Prado-Barragán, 2018).

This represents a significant amount of waste that is quite harmful due to the negative environmental effects, which result from the inappropriate residue management by the producer. Among the problems regarding the management of pineapple stubble in the field is the spread of the stable fly (*Stomoxys calcitrans*) (Solórzano et al., 2015). It occurs when pineapple stubble is reintegrated to the ground directly and while still fresh (green). This fly is considered a disease vector for people and for livestock on neighboring farms (Hernández-Chaverri & Prado-Barragán, 2018; Solórzano et al., 2015). Another problem caused by this stubble is the dry management carried out by the producer, in which the herbicide dimethyl-4,4'-bipyridyl, known as Paraquat, is applied. This herbicide presents cumulative toxicity that pollutes on a large scale the soils, thus affecting their future use and the environment, in general (Quesada-Solis et al., 2005). Once the chemical herbicide is applied, the area is burned and residues that remain are incorporated into the ground using harrows (Hernández-Chaverri & Prado-Barragán, 2018).

Thus, it is necessary to find ways for treating pineapple stubble to solve the problem of its disposal in the field. Besides, it is also necessary to aggregate value to pineapple stubble through biorefinery processes. Several investigations using this biomass have been carried out to manufacture a value-added product. Examples include the generation of biogas through anaerobic digestion (Arce-Hernández & Amador, 2014), biodiesel production (Marchena, 2019), bioethanol (Gil & Maupoey, 2018; Tropea et al., 2014), biochar for bioremediation of soils (Tang et al., 2013), fibers for the manufacture of composite materials (Hoque et al., 2018), among others. Also, pineapple stubble can be used as a precursor material for the production of activated carbon (Ahmed & Dhedan, 2012; Mahamad et al., 2015), a material that presents high surface area, porosity, and physicochemical stability and can be used for adsorption, purification, separation and catalysis processes (Achari et al., 2019; Yahya et al., 2015).

Production of activated carbon from lignocellulosic waste occurs primarily with two types of activation, chemical and physical. In physical activation, carbonization of the lignocellulosic precursor is carried out under an inert atmosphere and the resulting carbon from this step is subsequently activated through controlled partial gasification at high temperatures (ranges from 800 °C to 1100 °C), using as activating agents gases such as CO_2, air, steam, O_2, or a mixture of them (Olorundare et al., 2014; Yahya et al., 2015). On the other hand, in chemical activation, the precursor lignocellulosic material is directly impregnated with a chemical agent, such as H_3PO_4, H_2SO_4, HNO_3, $ZnCl_2$, NaOH, and KOH (González-García, 2018). For the production of activated carbon, the following factors should be considered: the ratio between the chemical activating agent and the lignocellulosic precursor material, type of activating agent, drying after impregnation and prior to carbonization (in many investigations, drying is carried out prior to carbonization at 100 ° C to favor impregnation and decomposition of the lignocellulosic matrix (Marsh & Rodríguez-Reinoso, 2006) and temperature of carbonization. Impregnation with the activating agent and carbonization-activation allows the dehydration and degradation of the lignocellulosic raw material and inhibit the formation of tar, ash, and other unwanted products during the carbonization process and therefore the production yield of activated carbon is promoted. (Ioannidou & Zabaniotou, 2007; Yahya et al., 2015). This activating agent-precursor undergoes a thermal carbonization process at a temperature range of 450 °C to 600 °C, in general (Molina-Sabio & Rodríguez-Reinoso, 2004). These conditions are less severe than those of physical activation.

The use of activated carbon for the removal of pollutants such as surfactants or dyes such as methylene blue in wastewater could be helpful for the preservation of aquatic ecosystems and human health. Hence, finding ways to remove these pollutants through the recovery of agricultural residues such as pineapple stubble stands as an alternative. Surfactants are common pollutants that can be found in water, which cause environmental problems such as inhibition of biological activity and foam generation; In general, wastewater treatment plants are not designed for the treatment of surfactants (Gil et al., 2012). It is a consequence of population growth, which leads to a substantial and progressive depletion and contamination of the water resource (Barrantes & Alfaro, 2016).

The objective of this research is to produce activated carbon from pineapple stubble under reduced oxidation conditions, as well as to determine its effectiveness in the removal of methylene blue and sodium dodecyl sulfate anionic surfactant.

The novelty of the present work consisted in the elaboration of an activated carbon produced from an agricultural residue such as pineapple stubble, where it was determined that the intermediate step of drying the biomass prior to carbonization is not necessary, this saves time and energy during its production; in addition, the adsorption of surfactants was tested with the activated carbon produced.

2. Materials and methods

2.1. Biomass (pineapple stubble)

The pineapple stubble sample was provided by the Bioenergetic and Environmental Research Unit (UIBEA) of the Distance State University (UNED). It is a sample composed of several sub-samples of stubble collected in the cantons of San Carlos (10 ° 35'53.6 "N 84 ° 29'59.5" W) and Los Chiles (10 ° 49'52.7 "N 84 ° 42'33.1" W) from Costa Rica, between the months of January-December 2018. It was preserved at a moisture level lower than 10%, in hermetic packaging, and out of the reach of light. Particle size was smaller than 8 mm. Moisture verification was carried out at (105 ± 3) ° C, for 4 h (Sluiter et al., 2008).

2.2. Preparation of activated carbon

To produce activated carbon, three factors were studied: activating agent [zinc chloride (Sigma-Aldrich, 98%) at 30% m/m and phosphoric acid (Quimar, 85%) at 30% v/v], activating agent (mL), and precursor (g) ratio (2:1 and 4:1) and the use or not of a drying stage prior to carbonization (dried for 24 h (103 ± 3) °C). Subsequently, the impregnated sample was placed in a crucible with a lid and its carbonization was carried out in a muffle (Thermolyne 1500) at an activation temperature of 600° C for 1.5 h. Once the sample is cooled, it is removed from the muffle, and washes were performed with approximately 900 mL of distilled water. Finally, the activated carbon was dried for 1 h (103 ± 3) °C, had its mass weighed, and was stored under normal laboratory conditions inside a plastic container for later use.

A 2^3 factorial design was proposed, with triplicates, from the factors and levels mentioned above. Table 1 shows the 2^3 factorial design matrix with the variables and their respective levels.

Table 1. Factorial design 2^3 with their respective variables and levels studied (interaction matrix).

Treatment	(A) Activating Agent	(B) Impregnation Ratio Activating agent (mL): precursor (g)	(C) Presence of drying prior to carbonization
1	$ZnCl_2$	2:1	No
2	H_3PO_4	2:1	No
3	$ZnCl_2$	4:1	No
4	H_3PO_4	4:1	No
5	$ZnCl_2$	2:1	Yes
6	H_3PO_4	2:1	Yes
7	$ZnCl_2$	4:1	Yes
8	H_3PO_4	4:1	Yes

Activated carbon production yield was chosen as the response variable. After performing the statistical analysis using the Statsolver software, the following equation was proposed for the model:

$$\%Y = 58.6 + 8.37 * X_A + 0.05 * X_B - 0.94 * X_C - 3.6 * X_{AB} - 0.19 * X_{AC} - 0.98 * X_{BC} - 0.34 * X_{ABC} \quad (1)$$

And the production yield was obtained using the following equation:

Where:

$\% Y$: activated carbon yield, %

m_{ac}: final weight of activated carbon produced, g

m_{rast}: initial weight of precursor, g

2.3. Infrared spectroscopy

The structure of the activated carbons obtained was characterized. Then, it was compared to the infrared spectrum of untreated pineapple stubble and the differences were observed. The equipment used was a Nicolet iS50 Thermo Scientific FT-IR infrared spectrophotometer, sampling with ATR accessory with diamond cell. For determinations, a range between 400 cm^{-1} and 4000 cm^{-1}, with a resolution of 4 cm^{-1}, was used. (Mahamad et al., 2015) Per analysis, 48 scans were done. This analysis was carried out in the specialized laboratory Instrumental Analysis Nucleus (NIA) of the UNED.

2.4. Moisture and ash determination

Pineapple stubble moisture and ash percentages were determined using ASTM E1756-08 and ASTM E1755-01, respectively. For the activated carbons produced, the ASTM D286 7-09 and ASTM D2866-11 standards were respectively used.

2.5. Elemental analysis

The CHNS content of the samples was determined using Thermo Scientific Flash Smart equipment from the Chemical Engineering Laboratory of the University of Costa Rica (UCR), using a 3-point calibration curve and BBOT as standard. The O content was calculated by difference. Combustion took place at 950 °C and helium was used as stripping gas. The amount of sample for each analysis was between 3-4 mg and 8-10 mg of vanadium pentoxide was added to the sample as a catalyst. Analysis of a blank sample was done prior to building the calibration curve and analyzing the samples. Samples and catalysts were placed in tin capsules.

2.6. X-ray fluorescence analysis

X-ray fluorescence analysis was performed to determine the chemical composition of activated carbons. 8 grams of the activated carbon sample were weighed and placed in the sample holder, which was introduced into the Bruker model S8Tiger WDXRF analyzer, where the X-rays were irradiated under a helium atmosphere.

2.7. Nitrogen adsorption analysis

The BET surface area, total pore volume, and average diameter for activated carbons were determined using the Autosorb iQ gas sorption analyzer, version 5.20.17081, from the Center for Electrochemistry and Chemical Energy (CELEQ) of the University of Costa Rica (UCR). Nitrogen adsorption-desorption isotherms were carried out at 77.350 K.

2.8. Scanning electron microscopy (SEM)

The morphology of the activated carbon produced was visualized with a Scanning Electron Microscope (SEM) model S-3700N, serial number 371238-03, with a voltage of 15,000 V at the Center for Research in Microscopic Structures (CIEMIC) of the UCR. The samples were mounted on a metal base, using a double contact tape which was used to adhere the sample to the metal base plate. The sample was coated prior to SEM analysis with a layer of gold.

2.9. Methylene blue adsorption

A standard solution of methylene blue ($C_{16}H_{18}N_3SCl$, Merck) of a concentration of 1000 mg/L was prepared with distilled water. The standard solution was stored in an amber bottle at room temperature before being used. Concentration standards between 0 and 12 ppm were prepared from the standard solution, and the calibration curve of absorbance vs. concentration was obtained by UV-VS spectrophotometry (Turner SP-870) at 660 nm with an R^2 value of 0.998. Adsorption tests were performed using an initial concentration of methylene blue of 400 mg/L, 0.5 g of activated carbon, and 50 mL of solution (Mahamad et al., 2015). These tests were held in a 250 mL beaker, using a magnetic stirrer template (Cole Palmer). To define the adsorption time (1 h) and the stirring speed (500 rpm), an initial test of adsorption capacity was done using the activated carbon produced from zinc chloride, at a 4:1 ratio and without drying. From this early result, it was built a curve of adsorption capacity of methylene blue q_f (mg/g) vs time (min).

To determine if there is a statistical difference concerning the adsorption of methylene blue between the different factors and their interrelationships, a 2^3 factorial statistical design, with triplicates, was proposed for each of the different activated carbon treatments shown in Table 1. The removal percentage of methylene blue was chosen as the response variable. The following equation was obtained for the model:

$$\%RAM = 99.25 - 0.69 * X_A + 0.56 * X_B + 0.54 * X_{AB} \quad (2)$$

The percentage removal of methylene blue was calculated as follows:

$$\% RAM = \frac{(Cn_i - Cn_f)}{Cn_i} * 100 \quad (3)$$

Where:

$\% RAM$: percentage removal of methylene blue, %

Cn_i: initial concentration of methylene blue, mg/L

Cn_f: final concentration of methylene blue after adsorption, mg/L

2.10. Activated carbon depletion

To determine the depletion of activated carbon (without regeneration process) activated carbon produced through treatment 3 ($ZnCl_2$, at a 4:1 ratio and without drying) was used. For such, different reuse cycles of activated carbon were performed during the adsorption of a solution containing 400 ppm of methylene blue as initial concentration. The final concentration of methylene blue was measured at the end of each cycle. A maximum concentration of 5 ppm was used as reference since this is the maximum limit allowed by the legislation on the discharge and reuse of wastewater in Costa Rica for methylene blue active substances (MINAE, 2007). Adsorption time was 1 h, stirring speed was 500 rpm, and 50 mL of solution and the same 0.5 g of activated carbon were used for each of the cycles.

2.11. Surfactant adsorption

Surfactant concentration was determined using the methodology of Maldonado (2008), which is an adaptation of the technique described by the American Public Health Association (APHA) & American Water Works Association (AWWA) (2005), specifically the 5540C standard for anionic

surfactants as methylene blue active substances. Activated carbon produced with zinc chloride, activating agent (mL), and precursor (g) of 4:1 and without previous drying was tested. Sodium dodecyl sulfate anionic surfactant solutions of 10 mg/L and 200 mg/L were prepared to test the adsorption of the activated carbon produced (Braga & Varesche, 2014; Wiel-Shafran et al., 2006). Similarly, the adsorption of residual gray water from a washing machine was carried out, after washing clothes using a commercial detergent. In both cases, the same adsorption conditions previously used for the adsorption of methylene blue were used.

3. Results and discussion

3.1. Production yield of activated carbon

The highest yields concerning the production of activated carbon, and using H_3PO_4, were achieved with treatments 2 and 6, with yields of 70.3% and 70.7% respectively; while using $ZnCl_2$ as activating agent, the highest yields were achieved with treatments 3 and 7, with corresponding yields of 55.3% and 52.5% respectively. Average production performance and standard deviation results are shown in Figure 1:

Statistical analysis of variance of the 2^3 factorial design concluded that only the chemical activating agent used is significant for the production yield of activated carbon ($p < 0.05$). The use of H_3PO_4 leads to a higher production yield, corroborating previous studies (Daffalla et al., 2012; Liou, 2010).

The higher yield provided using phosphoric acid (H_3PO_4) is due to the dehydrating effect it has on cellulose, hemicellulose, and lignin present in stubble, which occurs during the heat treatment (carbonization). In this stage, according to the previous research of Molina-Sabio and Rodríguez-Reinoso (2004), crosslinking reactions, which provide mechanical stability and rigidity, are predominant; in addition, there is a subsequent reduction in the output of volatile organic matter and tars, which favors the production yield of activated carbon. Moreover, the lower acidity of zinc chloride, when compared to phosphoric acid, as well as the presence of phosphates, catalyze the degradation of lignin and cellulose, therefore leading to a higher yield when using phosphoric acid (Molina-Sabio & Rodríguez-Reinoso, 2004). Besides, the residual insoluble phosphorus that remains on the surface of the activated carbon, along with the cellulose that is not so easily degraded, act as a recalcitrant material to hydrolysis, which could also explain the higher yields when using H_3PO_4 as an activating agent (Zubir & Zaini, 2020).

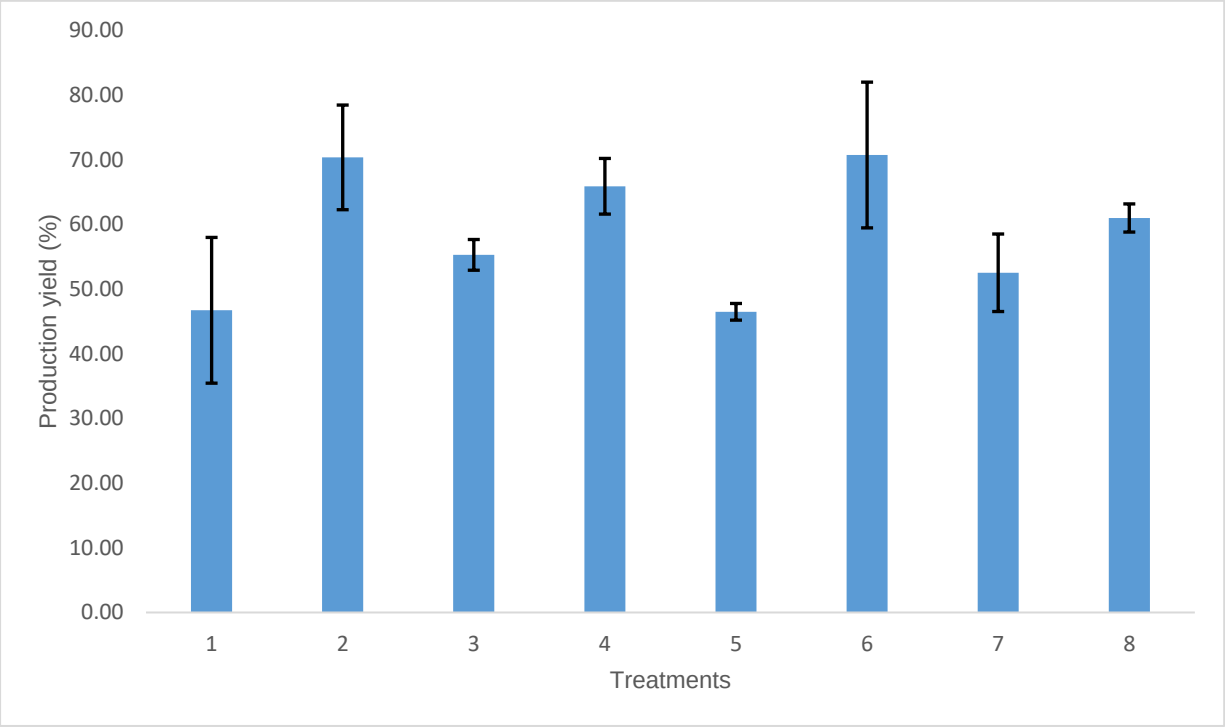

Figure 1. Results of the average production yield of activated carbon.

3.2. Methylene blue adsorption

Figure 2 shows the results for the removal percentage of methylene blue present in the water after adsorption using the activated carbons produced., From the statistical analysis, it could be observed that the effects A (chemical activating agent used), B (impregnation ratio activating agent (mL): precursor (g)), and the AB interaction are significant for the adsorption of methylene blue ($p < 0.05$).

From the significance of the AB interaction between the activating agent and the impregnation ratio used, it is possible to conclude that the activated carbon that provides higher adsorption under the studied conditions corresponds to the activated carbon produced using zinc chloride as activating agent at an impregnation ratio of 4:1 (treatments 3 and 7).

The investigated variable concerning drying prior to carbonization was not significant for adsorption of methylene blue. Therefore, to reduce costs associated with activated carbon production and the time it takes, treatment 3, in which activated carbon is produced without drying, was determined the best one. On the other hand, for activated carbon produced using phosphoric acid as activating agent, treatment 4 presented the best results. It favored the adsorption of methylene blue and save costs associated with the application of drying prior to carbonization. Besides no drying step, this treatment used an activating agent (mL): precursor (g) ratio of 4:1. Therefore, characterization analysis focused on activated carbons produced by treatments 3 and 4.

The adsorption of methylene blue on activated carbon can be assumed to follow the following four steps: 1) migration of the dye from the solution to the surface of the adsorbent, 2) diffusion of the dye through the boundary layer to the surface of the adsorbent, 3) adsorption of the dye to the active sites on the surface of the adsorbent and 4) intraparticle diffusion of the dye into the pores of the adsorbent (Hock et al., 2018).

The electrostatic attractions between the adsorbate and the adsorbent surface are a factor that can also affect the adsorption of methylene blue since methylene blue dissociates in water as a cationic molecule. Therefore, a cationic adsorbate will be more attracted to the surface of activated carbon when this surface is negatively charged, as is the case with activated carbons produced with zinc chloride and phosphoric acid (Altenor et al., 2009).

Figure 3a shows the methylene blue solution with a concentration of 400 ppm and Figure 3b shows the adsorption effect of the activated carbon produced by treatment 3 ($ZnCl_2$, a ratio of 4:1 and without drying prior to carbonization).

The difference of color present in the solution can be noticed, the initial concentration of methylene blue was 400 ppm, and after adsorption with the activated carbon produced by treatment 3 the methylene blue concentration was 0.179 ppm.

Table 2 presents a summary of the average percentages for production yield of activated carbon and methylene blue removal for each of the treatments performed.

Table 2. Methylene blue adsorption and production performance results after average adsorption and their respective standard deviations.

Treatment	Production yield of AC/(%)	MB removal percentage /(%)
1	46.70 ± 9.20	99.89 ± 0.01
2	70.30 ± 6.60	97.46 ± 0.12
3	55.30 ± 1.94	99.96 ± 0.06
4	65.90 ± 3.51	99.66 ± 0.25
5	46.50 ± 1.05	99.96 ± 0.01
6	70.70 ± 15.28	97.46 ± 0.15
7	52.50 ± 4.89	99.95 ± 0.06
8	61.00 ± 1.77	99.67 ± 0.08

*AC: activated carbon, MB: methylene blue

Figure 4 shows the relationship obtained for the two main response variables evaluated in the experimental design: the production yield of activated carbon and methylene blue removal. Treatments corresponding to the use of H_3PO_4 as activating agent have a higher production yield, however, they resulted in a lower methylene blue removal performance. It can be seen, regarding the even treatments, that treatments 2 and 6 correspond to the use of H_3PO_4 as an activating agent and that an impregnation ratio of 2:1 promotes lower removal of methylene blue when compared to 4:1 ratios (treatments 4 and 8), using the same activating agent. Likewise, it is observed that the odd treatments, which correspond to the use of $ZnCl_2$ as activating agent, resulted in lower yields of activated carbon production; however, at the same time, they promoted higher methylene blue removal. Characterizations of the activated carbons, presented below, allowed a better understanding of the observed behaviors.

Table 3 displays the adsorption results for the different activated carbon reuse cycles (depletion of activated carbon without regeneration) for treatment 3, with $ZnCl_2$ as activating agent, a ratio of 4:1, and without prior drying. Higher final concentrations of methylene blue were obtained each time by reusing activated carbon (after each adsorption cycle of 1 h) for adsorption of a new 400 ppm solution. This occurs due to more adsorption runs and an increase of competition between the methylene blue molecules, which leads to a decrease in the number of active sites (pores) available, thus hindering the methylene blue adsorption and, therefore, decreasing removal efficiency.

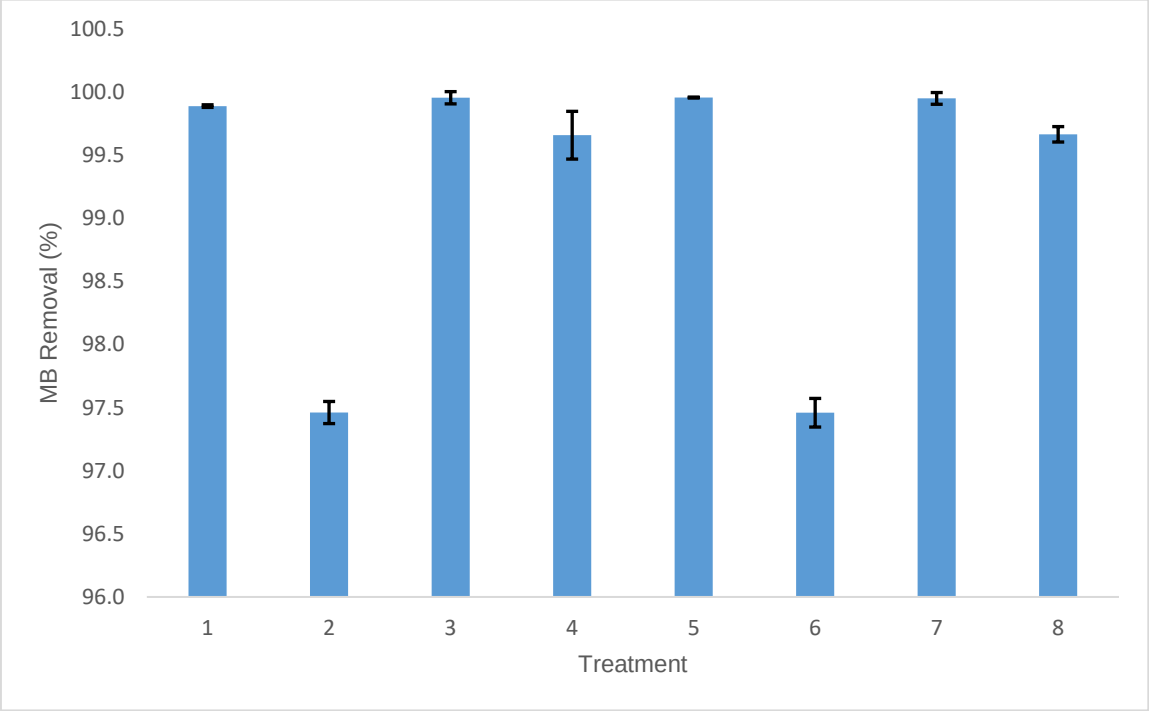

Figure 2. Results of the average percentage of methylene blue adsorption removal.

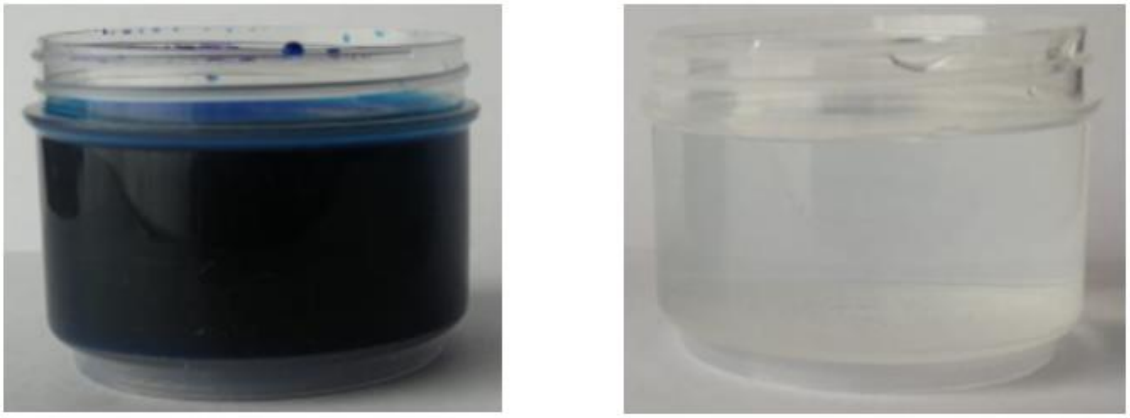

(a) (b)

Figure 3. (a) Solution before adsorption 400 ppm of methylene blue initial concentration. (b) Solution after adsorption with activated carbon produced by treatment 3 ($ZnCl_2$, a ratio of 4:1 and without drying prior to carbonization).

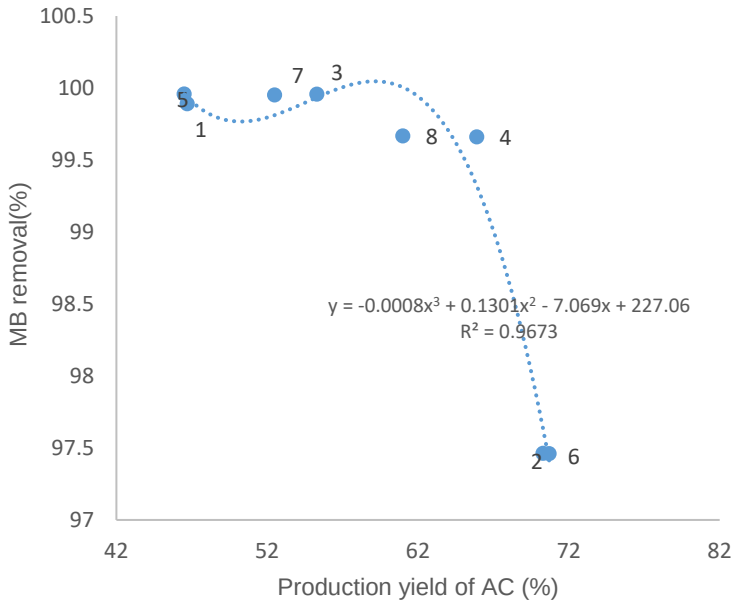

Figure 4. Correlation between the yield percentage and the percentage removal of methylene blue.

Table 3. Results for methylene blue adsorption for the different reuse cycles of activated carbon.

Metric	Adsorption cycles			
	1	2	3	4
Absorbance (adim)	0.03	0.15	0.59	1.84
Final concentration (ppm)	0.19	0.95	3.68	11.45
MB removal (%)	99.95	99.76	99.08	97.14
Adsorption capacity, q (mg/g)	39.98	39.91	39.63	38.86

After three cycles, a final concentration of methylene blue of 3.68 ppm was obtained. It is below the value used as a reference which corresponds to the limit allowed by the legislation for active substances to methylene blue (5 ppm) in Costa Rica. After the fourth cycle, a concentration of 11.45 ppm was obtained, which exceeds the reference value of 5 ppm. It was observed a decrease in the adsorption capacity of activated carbon from 39.98 mg/g to 38.86 mg/g after 4 cycles of use without regeneration.

3.3. FTIR spectra for the produced activated carbon samples and the pineapple stubble

In Figure 5, the spectrum of raw pineapple stubble (purple-fuchsia color) is displayed, without any treatment. The other spectra correspond to the triplicates of treatment 1 ($ZnCl_2$ as activating agent, impregnation ratio of 2:1, and no drying prior to carbonization). It was observed that there is a notorious peak at 3309 cm^{-1} for pineapple stubble, which corresponds to an O-H hydroxyl group. Close to that peak, another one can be seen, at 2917.15 cm^{-1}, which corresponds to a vibration of the C-H bond. It is noted that the spectrum of the produced activated carbons do not contain these peaks, indicating that the hydrogen present in the lignocellulosic matrix of the stubble is eliminated during activation and carbonization processes, a situation that was also observed in the research of Mahamad et al. (2015).

Furthermore, it is possible to observe characteristic peaks of lignocellulosic materials, such as the one at 1625.33 cm^{-1}, which is associated with aromatic skeletal vibrations mainly attributed to lignin. Peaks at approximately 1440 cm^{-1}, 1372.03 cm^{-1}, 1315 cm^{-1}, and others that are close to them are associated with torsional vibrations of the -CH_2, C-H, and C-O groups of the aromatic rings, respectively (Nicolaas et al., 2019). The peak at 1244.72 cm^{-1} belongs to the C – O stretching bond of lignin, while between 1030.08 cm^{-1}, and 1160 cm^{-1}, there are peaks corresponding to absorptions attributed to the deformation of the oscillating vibration C – H and to the

stretching of the skeleton of the pyranose ring C–O–C (Nicolaas et al., 2019). The high peak at 1030.08 cm^{-1} can also be attributed to the C – O bonds, the C = C double bond, and the C – C–O stretch present in lignin, cellulose, and hemicellulose (Xu et al., 2013).

It could be observed, from the spectra obtained for the replicas of this treatment, that almost all the previous peaks decreased. This indicates that the multiple bonds of the starting material were significantly eliminated. Therefore, the number of functional groups present in dried pineapple stubble is reduced after carbonization, due to the decomposition of the complex lignocellulosic matrix into simpler compounds or groups.

Similarly, to the spectrum observed for treatment 1, in Figure 6, which refers to treatment 2, it can be seen, for the replicas, that there is also a decrease in the peaks, compared to those for pineapple stubble. This implies a lower concentration of functional groups. Regions of multiple bonds and those corresponding to vibrations caused by sp^2 hybridization in C-H bonds were also eliminated. These results suggest that phosphoric acid serves well as an activating agent to produce activated carbon. When using both phosphoric acid and zinc chloride, decomposition of the lignocellulosic matrix was observed and, consequently, simpler carbonaceous structures were formed.

Since carbonization was held at 600 °C and for a longer time than in the previous investigation by Mahamad et al. (2015), a decrease in the number of functional groups was already expected. This decomposition of the primary groups on the surface of activated carbon, at a high temperature, leads to the formation of new pores (Hock et al., 2018).

3.4. Moisture and ash

Table 4 displays the moisture and ash results obtained for pineapple stubble and activated carbon (treatments 1 to 4) which are the treatments produced without drying prior to carbonization.

Activated carbons produced in the present study present high moisture levels when compared to other investigations, such as Mahamad et al. (2015). This is mainly because, after carbonization and washing with distilled water, the activated carbons were left for drying for only one hour, at 103 °C. It is a short time, compared to other works. In these, after washing, activated carbon is left for drying for 6 hours or a whole day. However, it should be noted that this one-day drying time is costly, hence, to keep on working with the purpose of saving energy during the drying stage, time was set to only one hour and at 103 °C. However, the high levels of moisture did not affect the adsorption capacity of the activated carbon under the studied conditions.

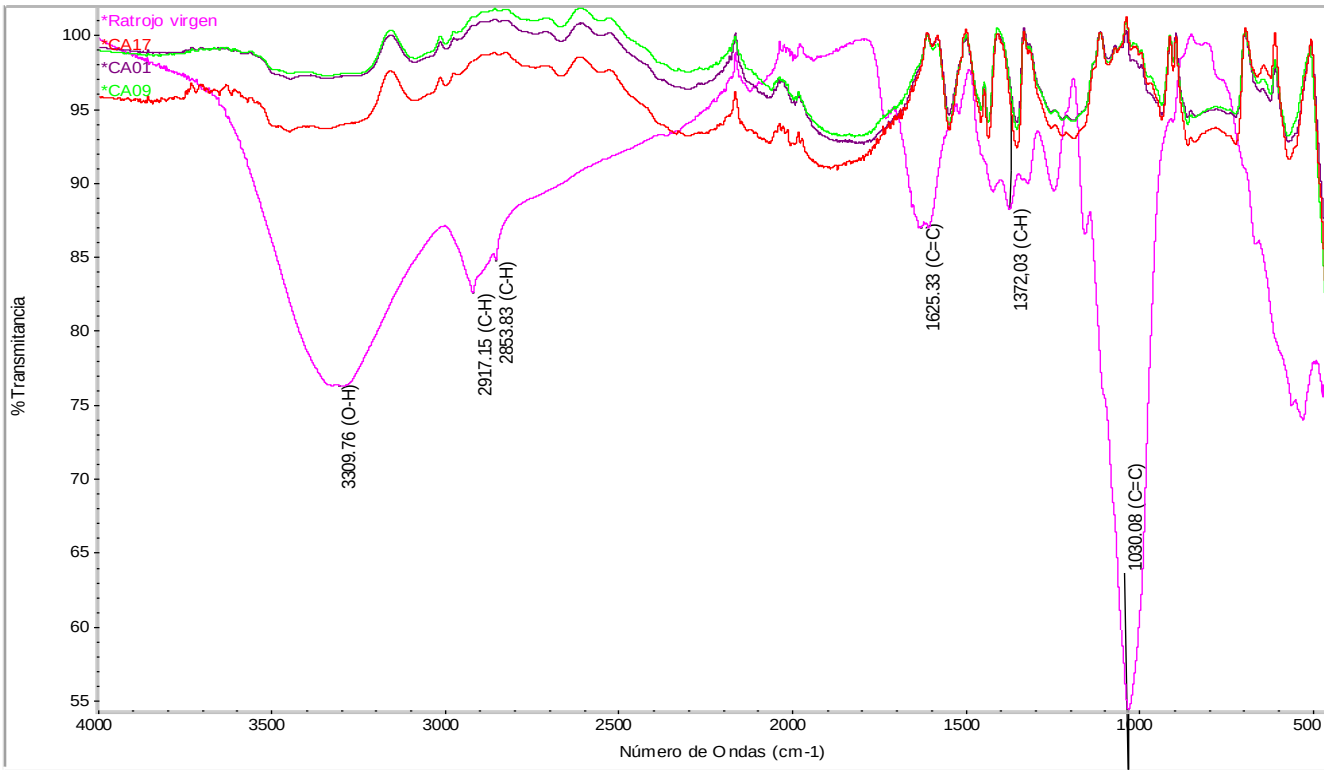

Figure 5. FTIR spectrum of treatment 1 corresponding to $ZnCl_2$, a ratio of 2:1 and without drying.

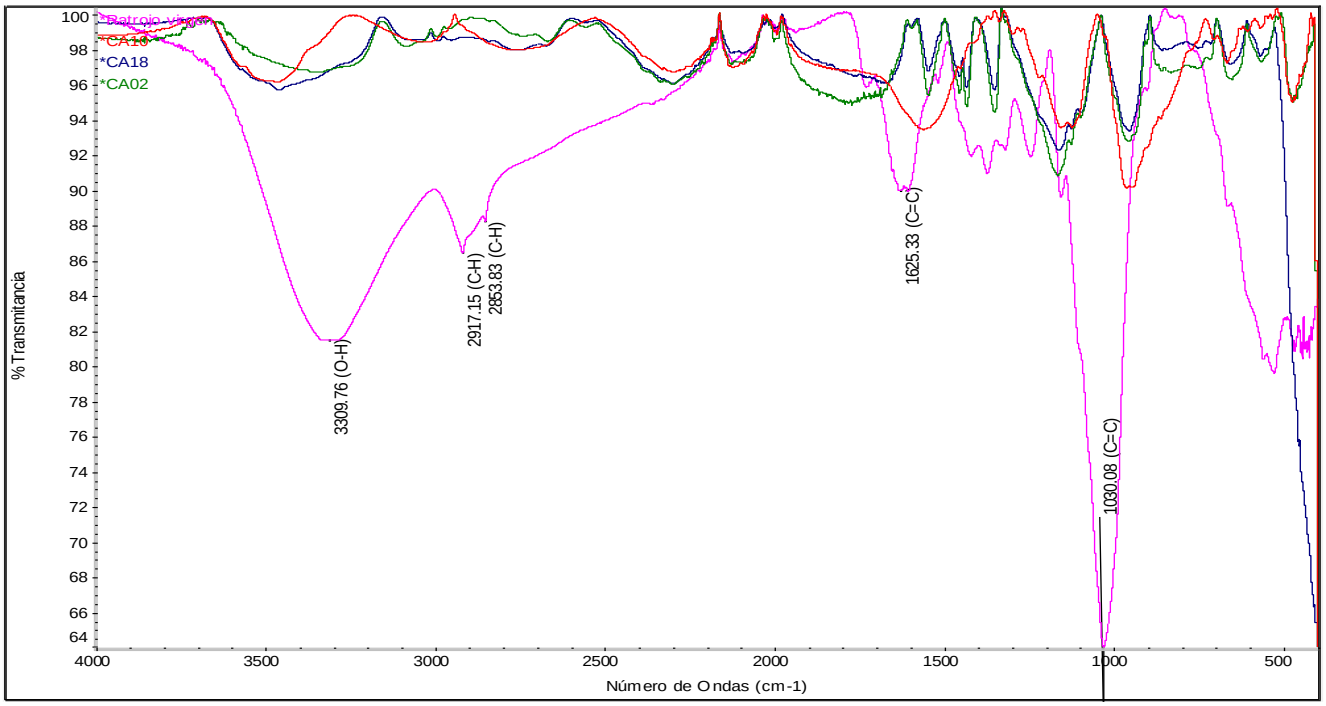

Figure 6. FTIR spectrum of treatment 2 corresponding to the use of H_3PO_4, a ratio of 2:1 and without drying.

Table 4. Moisture and ash results for pineapple stubble used as raw material and for activated carbons produced with the first 4 treatments.

Sample	Moisture (%)	Ash (%)
Pineapple Stubble	10.90	11.36
AC- 1	22.87	25.36
AC- 2	16.13	28.43
AC- 3	22.15	21.65
AC- 4	16.81	21.71

*AC: activated carbon

For activated carbons produced with a lower impregnation ratio between activating agent (mL) and precursor (g) (2:1), higher amounts of ash were obtained, once compared to cases in which a ratio of 4:1 was used, demonstrating the effect of this ratio on the process. Higher volumes of the activating agent inhibit excessive degradation of the stubble since the stubble is impregnated to a greater extent. Therefore, carbonization is favored, resulting in less ash formation (Joseph et al., 2006; Yahya et al., 2015).

It should be noted that treatment 2 (2:1 ratio using H_3PO_4) resulted in the highest levels of ash. Coincidentally, this treatment provided a higher production yield and a lower adsorption capacity. Other investigations have indicated that high levels of ash in the activated carbon decrease its adsorption: this occurs because the active sites are covered by the ashes, not allowing methylene blue molecules to adsorb on them (Ortega et al., 2017)

3.5. Elemental analysis

Table 5 displays the results of the elemental analysis for the activated carbons from treatment 3 ($ZnCl_2$, a ratio of 4:1 and without prior drying) and treatment 4 (H_3PO_4, a ratio of 4:1 and without prior drying). These treatments correspond to the produced activated carbons that presented the highest adsorption of methylene blue, for each of the activating agents used. Activated carbon produced by treatment 3 presents a higher carbon content than that of the precursor material. This indicates that after impregnation of the precursor with $ZnCl_2$, followed by activation, carbonization was favored.

The opposite occurred with activated carbon produced by treatment 4, which presents a lower carbon content after activation-carbonization. Such decrease might be due to the nature of the activating agent (H_3PO_4) and its interaction with the precursor material: the presence of heteroatoms in the biomass promotes the H_3PO_4 catalytic effect on the volatilization of the material and on the C-O-C and C-C bonds, resulting in the decrease of the carbon content (Ravichandran et al., 2018). Decreases in the hydrogen and oxygen contents were also observed, after activation-

carbonization of precursor material; this is associated with decreases in the number of functional groups and multiple bonds originally present in the complex lignocellulosic matrix of pineapple stubble and corroborates results obtained through the FTIR analysis.

Table 5. Elemental analysis of activated carbons from treatments 3 and 4 and of pineapple stubble (dry basis).

Element	Pineapple Stubble	AC-3 ($ZnCl_2$)	AC-4 (H_3PO_4)
N (%)	1.134	1.175	0.954
C (%)	37.706	42.223	34.545
H (%)	4.972	1.968	1.677
S (%)	0.251	0.256	0
O (%)	44.575	32.725	41.113

3.6. X-ray fluorescence

Table 6 summarizes the surface chemical composition of the activated carbon in its oxide form. For activated carbon produced through treatment 3, ZnO predominates with 64.71%, followed by Cl with 8.11% and SiO_2 with 7.82%. Treatment 3 corresponds to the production of activated carbon using $ZnCl_2$ as activating agent, which explains why elements such as Zn and Cl predominate. Elements such as Al, Mg, P, Fe, and S in their oxide form are also present, in a range between 4.10 % to 3.36%, while traces of elements such as Ca, Ti, Cu, Mn, Cr, or Zr are also reported. The presence of these elements might be associated with the cultivation of pineapple, in which the quality and quantity of fertilizer used, influence the concentration of minerals absorbed by the plant. In addition, the way the soil is managed could also influence the presence of particles or minerals (Braga et al., 2015).

Regarding activated carbon produced through treatment 4, it is observed that the predominant oxide is P_2O_5 (82.4%) followed by SiO_2 (11.2%). Since this activated carbon was produced using H_3PO_4, it was expected phosphorus, in its P_2O_5, to be the main component detected. Such high amount of P_2O_5 on the surface of the activated carbon could affect adsorption, resulting in a lower adsorption performance when compared to activated carbons produced using $ZnCl_2$. The research by Zbair et al. (2018) indicated that activated carbons with high phosphorus (P) content achieved lower adsorption yields of methylene blue than activated carbons with lower P content.

Table 6. Normalized results of the chemical composition of the surface of the activated carbon samples determined by X-ray fluorescence.

Element/Compound	Treatment 3: $ZnCl_2$	Treatment 4: H_3PO_4
ZnO	64.71 %	-
Cl	8.11 %	-
SiO_2	7.82 %	11.2 %
Al_2O_3	4.10 %	1.42 %
MgO	3.97 %	0.549 %
P_2O_5	3.54 %	82.4 %
Fe_2O_3	3.36 %	1.64 %
SO_3	3.36 %	0.125 %
K_2O	-	1.59 %
CaO	0.680 %	0.798 %
TiO_2	0.215 %	0.116 %
CuO	385 ppm	91.1 ppm
MnO	243 ppm	348 ppm
Cr_2O_3	115 ppm	106 ppm
ZrO_2	56 ppm	124 ppm

3.7. Nitrogen physisorption analysis

Nitrogen physisorption analysis was done for the corresponding samples of the treatments that provided the highest adsorption of methylene blue. These were treatments 3 and 4, both of which worked with an impregnation ratio of 4:1 and without drying prior to carbonization, the difference being the activating agent used: zinc chloride for treatment 3 and phosphoric acid for treatment 4.

Figure 7 shows the nitrogen adsorption isotherm obtained for the activated carbon produced by treatment 4 (H_3PO_4, a ratio of 4:1 and without drying). The red-colored curve represents adsorption, while the blue-colored curve, desorption. This isotherm tends to a type IV isotherm with a type H3 hysteresis cycle, according to the examples presented by IUPAC. This isotherm is characteristic of activated carbons with mesopores of disordered structure (Thommes et al., 2015).

Figure 8 shows the isotherm for the activated carbon produced by treatment 3 ($ZnCl_2$, a ratio of 4:1 and without drying). This isotherm tends to a type IV isotherm with a type H4 hysteresis cycle, according to the examples presented by IUPAC (Thommes et al., 2015). It is characteristic of activated carbons with micro and mesopore structures. It can be noticed, from the points close to a relative pressure of zero, that there is an initial volume for adsorption, which is indicative of the presence of micropores in the structure.

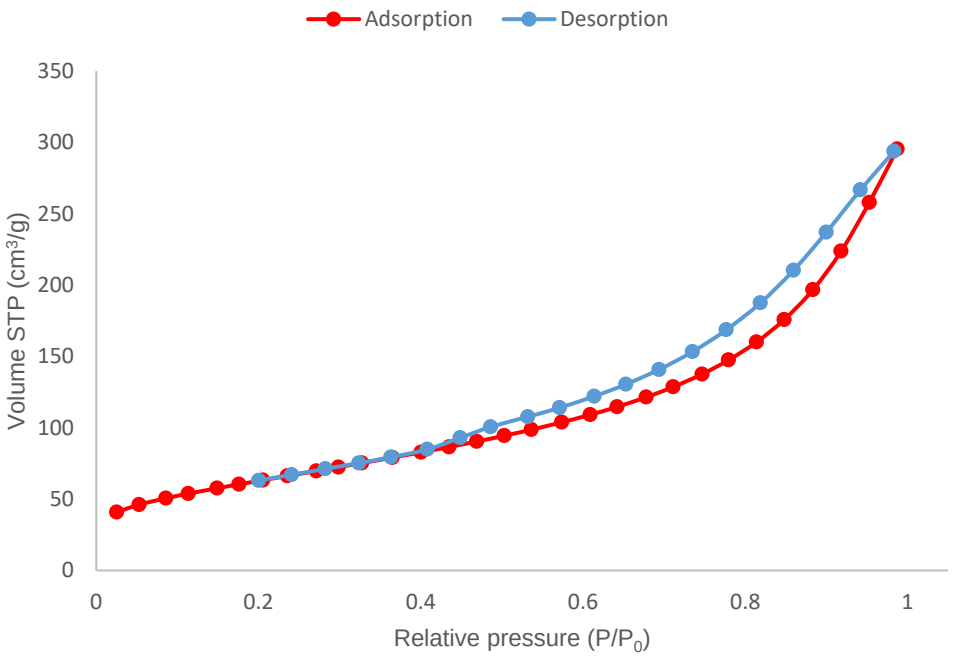

Figure 7. Nitrogen adsorption isotherm for the activated carbon sample produced with treatment 4 using H_3PO_4 as activating agent, at a ratio of 4:1.

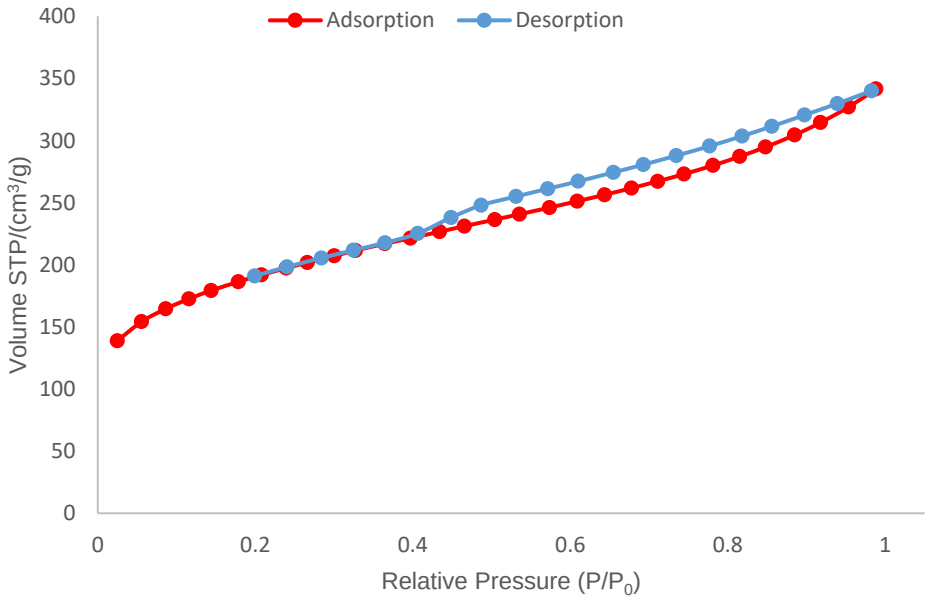

Figure 8. Nitrogen adsorption isotherm for the activated carbon sample produced with treatment 3 using $ZnCl_2$ as activating agent at a ratio of 4:1.

The highest surface area, as well as the highest pore volume amongst the activated carbon produced, was achieved using zinc chloride as activating agent (Table 7). This indicates that, for this type of activated carbon, there is a high number of active sites in which methylene blue is retained. And it is the reason why activated carbons produced with zinc chloride provided better adsorption results than those produced using phosphoric acid.

Table 7. Results obtained from the characterization of the BET surface area and pore characteristics of activated carbons.

Sample	BET surface area (m^2/g)	Total pore volume (cm^3/g)	Average pore diameter (nm)	Observation
AC-3 ($ZnCl_2$)	685.6	0.53	3.1	Presents micro and mesopore structures.
AC-4 (H_3PO_4)	228.3	0.46	8.0	Presents disordered pore structures.

The difference between the surface areas for each activated carbon produced using the activating agents H_3PO_4 and $ZnCl_2$ is related to the different activation mechanisms. It has been proposed that the activation of phosphoric acid is carried out through the formation of cross-linked structures in the form of phosphate esters, which are directly related to the development of porosity (Jagtoyen & Derbyshire, 1998). At a temperature of 600 °C occurs a breakdown of these cross-linked structures, causing contraction and reduction in the porosity development (Donald et al., 2011). In contrast, the activation mechanism of zinc chloride is believed to be more related to the "swelling" effect of the lignocellulosic matrix of pineapple stubble caused by $ZnCl_2$. This results in a breakdown of the lateral bonds of the molecules of cellulose and consequent creation of interspaces, allowing easier access of the activating agent to the interior of the biomass structure (Donald et al., 2011). In other words, the activating agent acts as a template for the subsequent formation of microporosity, later obtained through the activated carbon washing, in which remnants of zinc chloride are eliminated, thus creating microporosity (Molina-Sabio & Rodríguez-Reinoso, 2004).

This microporosity on the sample prepared with zinc chloride is related to the size of this salt molecule. However, this is not the case for phosphoric acid, since there is no specific molecule of H_3PO_4, but a mixture of molecules from H_3PO_4 and $H_4P_2O_5$ to $H_{13}P_{11}O_{34}$, in the proportion predicted by the liquid-vapor phase diagram for P_2O_5-H_2O mixtures, resulting in heterogeneity in terms of pore size (Molina-Sabio & Rodríguez-Reinoso, 2004). Additionally, since phosphoric acid is a stronger acid than zinc chloride and considering that a 4:1 ratio is high, a more intense chemical attack occurs on the precursor, which contributes to the average diameter of the pores of this activated carbon: 8 nm, notably larger than that of the activated carbon sample prepared with zinc chloride (3.1 nm.).

Therefore, according to the results obtained in this analysis and in agreement with Donald et al. (2011), it can be indicated that zinc chloride is more effective in the development of meso and microporous structures, which promote higher surface areas. Phosphoric acid, on the other hand, is more effective in the development of mesopores (disordered and heterogeneous), which lead to larger average pore diameters.

Table 8 compares the surface area results of the activated carbon produced in this investigation with predecessor work.

Table 8. Comparison of the surface area of activated carbons produced by chemical activation from different lignocellulosic precursors.

Raw lignocellulosic material	Chemical activating agent	BET surface Area (m^2/g)	Reference
Pineapple stubble	$ZnCl_2$	685.6	This work
	H_3PO_4	228.3	
Teak wood (*tectona grandis*)	H_3PO_4	688.54	(Cambronero, 2018)
Eucalyptus and pine seed husk and peach bone	H_2SO_4	358-418	(Rincón, 2016)
Eucalyptus seed husk	H_2SO_4	70-120	(Rincón et al., 2015)
	$ZnCl_2$	220-300	
Sisal (agave)	$ZnCl_2$	616	(Yu et al., 2015)
Eucalyptus seed husk	H_3PO_4	1027-2009	(Rincón et al., 2014)
Macadamia nut endocarp	$ZnCl_2$	600	(Pezoti Junior et al., 2014)
Cocoa pod husk	KOH	490	(Cruz et al., 2012)
	$ZnCl_2$	780	
African palm endocarp	H_3PO_4	391.71	(Bastidas et al., 2010)
Coffee residue	$ZnCl_2$	890	(Boudrahem et al., 2009)
Hazelnut bagasse	KOH	1642	(Demiral et al., 2008)
	$ZnCl_2$	1489	
Coconut fiber	$ZnCl_2$	540	(Macedo et al., 2008)
Sugarcane bagasse	H_3PO_4	320	(Giraldo-Gutiérrez & Moreno- Piraján, 2008)
Chestnut wood	H_3PO_4	783	(Gómez-Serrano et al., 2005)

3.8. Surfactant adsorption

Table 9 displays the results for the adsorption of surfactants in the activated carbon produced with treatment 3 ($ZnCl_2$ as activating agent, a ratio of 4:1 and without drying prior to carbonization).

Table 9. Adsorption results for surfactant sodium dodecyl sulfate and gray water collected after washing clothes with commercial detergent.

Metric	Sodium dodecyl sulfate solution	Sodium dodecyl sulfate solution	Gray water after washing with a commercial detergent
Initial MBAS concentration (mg/L)	10	200	136
Absorbance after adsorption (adim)	0.086	0.724	1.752
Final concentration (mg/L)	0.126	0.798	1.88
Removal Efficiency(%)	98.7	99.6	98.6

*MBAS: methylene blue active substances

The produced activated carbon presents efficient adsorption of sodium dodecyl sulfate solutions. For the same conditions used in the adsorption of methylene blue, at both scenarios a final concentration of methylene blue active substances lower than 1 mg/L was obtained. In Costa Rica, the maximum discharge limit of methylene blue active substances in sanitary sewers and receptor bodies is 5 mg/L (MINAE, 2007). Hence, the produced and evaluated activated carbon provided remarkably interesting results, within legislation limits.

Activated carbon proved to be effective in the adsorption of sodium dodecyl sulfate solutions. For both scenarios, a removal efficiency higher than 98 % was achieved. Similar results were obtained in the adsorption of gray water: a final concentration of 1.88 mg/L of methylene blue active substances was achieved, a value that is also below the allowed limit (5 mg/L) (MINAE, 2007). A removal percentage of 98.6 % was obtained, thus indicating effective adsorption of the anionic surfactants present in the residual gray water.

3.9. SEM analysis

SEM analysis is shown in Figure 9. In Figure 9 (a) it can be seen the different pores that compose the carbonaceous structure of the activated carbon produced using $ZnCl_2$ as activating agent (treatment 3). The structure is similar to that obtained in the work of Mahamad et al. (2015), which also used pineapple stubble and $ZnCl_2$. Porous structures can be attributed to the dehydration effect of $ZnCl_2$, the oxidation of organic compounds in the carbonization stage, and the fact that zinc chloride acts as a template for porosity formation. The SEM analysis confirms the results found in the BET analysis of surface area and porosity, from which it was concluded that the activated carbon produced with $ZnCl_2$ contains micro and mesopore structures.

In Figure 9 (b) (treatment 4, H_3PO_4 as activating agent and a 4:1 ratio), a clear difference in morphology can be noted. This activated carbon presents a more irregular porous structure and less porosity when compared to activated carbon produced by treatment 3 (Figure 9 (a)). It can also be seen that porous and cavities are not as defined or ordered. This corroborates results previously obtained in the BET analysis, in which it was indicated that the surface area and the total pore volume were lower for this activated carbon.

Activated carbon shown in Figure 9 (c) corresponds to the same treatment as that shown in (a), but after the adsorption process of methylene blue. There is a clear difference in the surface observed for this activated carbon in comparison with the observed for the same activated carbon without adsorption. A uniform layer that covers the carbonaceous structure after adsorption can now be seen. Also, pores are not as clearly distinguished as in Figure 9 (a). These results are similar to those reported by Mahamad et al. (2015) for the SEM analysis of activated carbon after adsorption of methylene blue. And suggest that methylene blue sticks to the surface of the activated carbon, thus saturating the pores.

The morphology of the activated carbon plays an important role in its adsorption capacity since characteristics such as the surface area or the pore size present determine whether the activated carbon is efficient or not for the adsorption of a certain pollutant. The greater the surface area present in the activated carbon, the greater the number of active sites available for adsorption. In the present work, it was demonstrated that the activated carbon produced with a higher surface area (treatment 3, $ZnCl_2$, ratio 4:1 and without prior drying) of 685.6 m^2/g, which also has a greater total pore volume had better adsorption than activated carbon produced by treatment 4 (H_3PO_4).

Another important factor to consider in the morphology of activated carbon that influences the adsorption of activated carbon is the size of the pore present since the presence of microporosity favors the adsorption of adsorbates such as methylene blue. This occurs because micropores have molecular dimensions (Sann & Adeeyo, 2016), therefore a small adsorbate molecule such as methylene blue will easily penetrate a pore that has a particular size. According to the physisorption analysis carried out, it was determined that the

activated carbon produced by treatment 3 has the presence of micropores, while in the activated carbon produced by treatment 4 the presence of mesopores predominates, therefore it is not surprising that activated carbon produced by treatment 3 showed better adsorption of methylene blue.

SEM analysis was also carried out for the activated carbon used in the adsorption of the surfactant sodium dodecyl sulfate. Results are shown in Figure 9 (d). On the surface of the carbonaceous structure, some particles can be observed, which could be remnants of zinc chloride or sodium dodecyl sulfate. However, a uniform layer is not observed on the surface of this activated carbon, as it was in Figure 9 (c). This could be attributed to the fact that 4 reuse cycles of activated carbon were performed during the adsorption of methylene blue, while activated carbon shown in Figure 9 (d) was used for surfactant adsorption only once.

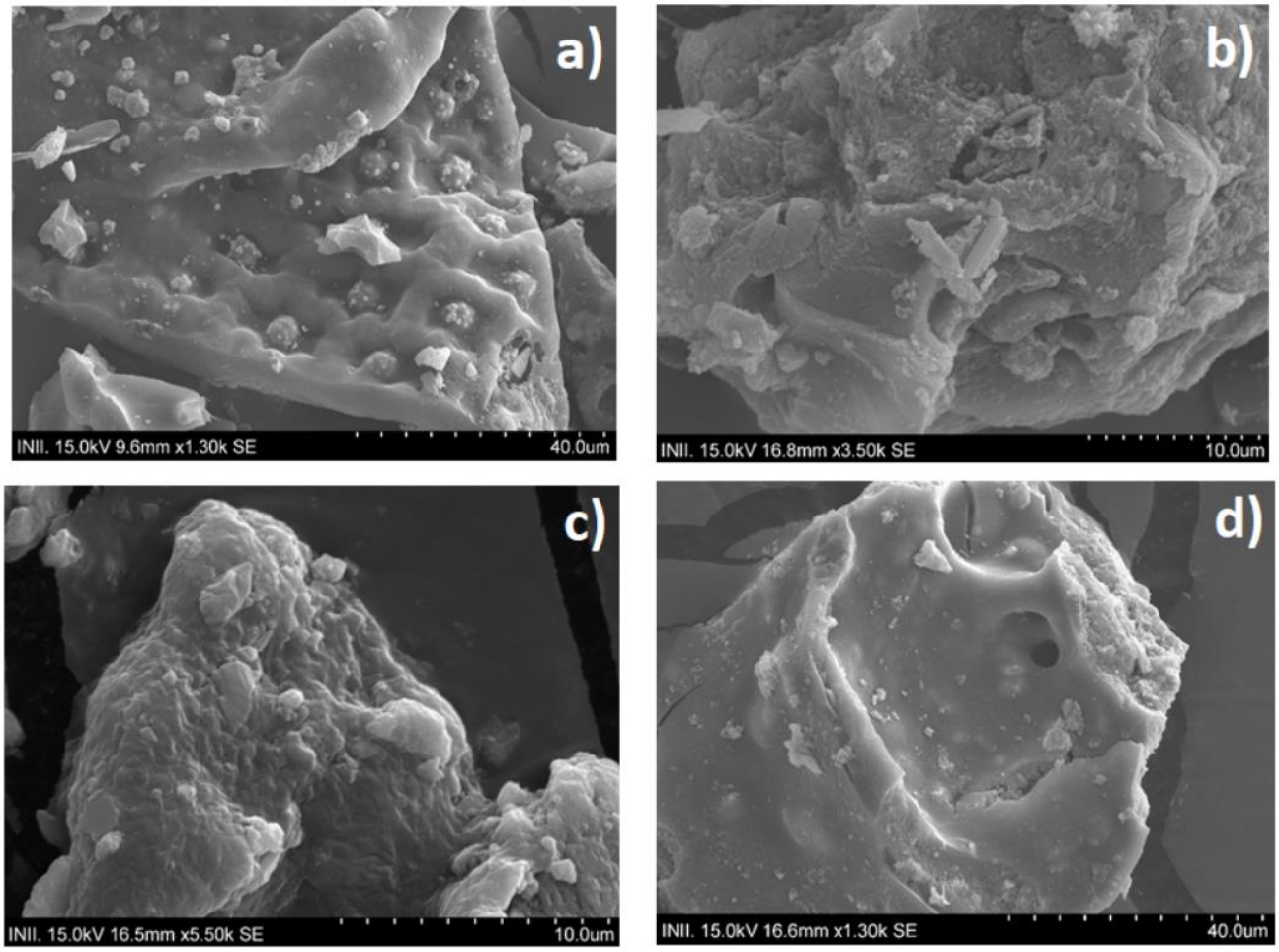

Figure 9. SEM of activated carbons: a) AC treatment 3 ($ZnCl_2$, 4:1 ratio), b) AC treatment 4 (H_3PO_4, 4:1 ratio), c) AC treatment 3 after the adsorption cycles of methylene blue, d) AC treatment 3 after the adsorption of sodium dodecyl sulfate

4. Conclusions

From a lignocellulosic agricultural waste such as pineapple stubble, it is possible to produce effective activated carbons, with appropriate surface area and pore volume and with the ability to adsorb methylene blue and surfactants. The statistical analysis concluded that the activating agent is the significant factor for the production of activated carbons, and it is favored when H_3PO_4 is used. Concerning the adsorption of methylene blue, it was found that the significant factors are the use of the activating agent, a ratio between the activating agent (mL) and the precursor (g), and interaction amongst both factors. $ZnCl_2$ was the activating agent that provided higher adsorption, while an impregnation ratio of 4:1 proved to be more efficient. Also, it was concluded that a drying step, prior to carbonization, did not have any significant effect on the adsorption of methylene blue. This is an interesting result, allowing for saving both time and energy during production.

Zinc chloride proved to be more effective in the development of microporous activated carbons with higher BET surface area and total pore volume. Phosphoric acid, on the other hand, is more effective in developing mesopores, and activated carbons produced using H_3PO_4 present a higher average pore diameter. Activated carbon produced using zinc chloride was highly effective regarding adsorption of both the anionic surfactant sodium dodecyl sulfate and the residual gray water from washing clothes with commercial detergent. Removal efficiencies were above 98% for both cases, achieving, for methylene blue active substances, concentration values below the maximum limit of 5 mg/L, according to the regulation of reuse and discharge of wastewater of Costa Rica.

Conflict of interest

The authors have no conflicts of interest to declare.

Acknowledgments

Special thanks to the Forest Resources Unit of the Engineering Research Institute, for providing the space and the laboratory equipment through which this research could be carried out; also, to the Instrumental Analysis Nucleus of the UNED, CELEQ, and CIEMIC for the characterizations carried out. In addition, thanks to the UCR School of Chemical Engineering for their collaboration during the development of the project.

References

Achari, V. S., Rajalakshmi, A. S., Jayasree, S., & Lopez, R. (2019). Surface Area and Porosity Development on Granular Activated Carbon by Zirconium: Adsorption Isotherm Studies. *Journal of Applied Research and Technology, 16*(3). https://doi.org/10.22201/icat.16656423.2018.16.3.719

Ahmed, M. J., & Dhedan, S. K. (2012). Equilibrium isotherms and kinetics modeling of methylene blue adsorption on agricultural wastes-based activated carbons. *Fluid Phase Equilibria, 317*, 9–14. https://doi.org/10.1016/j.fluid.2011.12.026

Altenor, S., Carene, B., Emmanuel, E., Lambert, J., Ehrhardt, J. J., & Gaspard, S. (2009). Adsorption studies of methylene blue and phenol onto vetiver roots activated carbon prepared by chemical activation. *Journal of Hazardous Materials, 165*(1–3), 1029–1039. https://doi.org/10.1016/j.jhazmat.2008.10.133

American Public Health Association (APHA), & American Water Works Association (AWWA). (2005). *Standard Methods for the Examination of Water and Wastewater* (21st ed.).

Arce, A., Hernández, C., & Amador, R. (2014). Determinación de la Cantidad y Composición de Biogás a partir de Rastrojo de la Piña (Ananas comosus) por medio de un sistema continuo a escala laboratorio. San José, Costa Rica: ICE Programa Biogas. 1–8.

Boudrahem, F., Aissani-Benissad, F., & Aït-Amar, H. (2009). Batch sorption dynamics and equilibrium for the removal of lead ions from aqueous phase using activated carbon developed from coffee residue activated with zinc chloride. *Journal of Environmental Management, 90*(10), 3031–3039. https://doi.org/10.1016/j.jenvman.2009.04.005

Bastidas, M., Buelvas, L. M., Márquez, M. I., Popular, U., & De, C. (2010). Activated Carbon Production from Carbonaceous Precursors of the Department of Cesar, Colombia. *Información Tecnológica, 21*(3), 87–96.

Braga, J. K., & Varesche, M. B. A. (2014). Commercial Laundry Water Characterisation. *American Journal of Analytical Chemistry, 05*(01), 8–16. https://doi.org/10.4236/ajac.2014.51002

Braga, R. M., Queiroga, T. S., Calixto, G. Q., Almeida, H. N., Melo, D. M. A., Melo, M. A. F., Freitas, J. C. O., & Curbelo, F. D. S. (2015). The energetic characterization of pineapple crown leaves. Environmental Science and Pollution Research, 22(23), 18987–18993. https://doi.org/10.1007/s11356-015-5082-6

CANAPEP. (2020). *Estadísticas, Cámara Nacional de Productores y Exportadores de Piña*. https://canapep.com/estadisticas/

Cruz, G., Pirila, M., Huuuhtanen, M., Carrion, L., Alvarenga, E., & Keisiki, R. (2012). Production of Activated Carbon from Cocoa (Theobroma cacao) Pod Husk. *Journal of Civil & Environmental Engineering, 2(2)*, 2–7. https://doi.org/10.4172/2165-784x.1000109

Cambronero Soto, C. A. (2018). *Producción y evaluación del uso de carbón activado como un coadyudante en la fertilización de los cultivos de cebolla.* [Proyecto de graduación, Universidad de Costa Rica]Repositorio del SIBDI-UCR

Demiral, H., Demiral, I., Tümsek, F., & Karabacakoğlu, B. (2008). Pore structure of activated carbon prepared from hazelnut bagasse by chemical activation. *Surface and Interface Analysis*. *40*(3-4), 616-619. https://doi.org/10.1002/sia.2631

Daffalla, S. B., Mukhtar, H., & Shaharun, M. S. (2012). Properties of activated carbon prepared from rice husk with chemical activation. *International Journal of Global Environmental Issues, 12*(2–4), 107–129. https://doi.org/10.1504/IJGENVI.2012.049375

Donald, J., Ohtsuka, Y., & Xu, C. C. (2011). Effects of activation agents and intrinsic minerals on pore development in activated carbons derived from a Canadian peat. *Materials Letters, 65*(4), 744–747. https://doi.org/10.1016/j.matlet.2010.11.049

Gómez-Serrano, V., Cuerda-Correa, E. M., Fernández-González, M. C., Alexandre-Franco, M. F., & Macías-García, A. (2005). Preparation of activated carbons from chestnut wood by phosphoric acid-chemical activation. Study of microporosity and fractal dimension. *Materials Letters, 59*(7), 846–853. https://doi.org/10.1016/j.matlet.2004.10.064

Giraldo Gutiérrez, L., & Moreno Piraján, J. C. (2008). Pb(II) and Cr(VI) adsorption from aqueous solution on activated carbons obtained from sugar cane husk and sawdust. *Journal of Analytical and Applied Pyrolysis, 81*(2), 278–284. https://doi.org/10.1016/j.jaap.2007.12.007

Gil, L. S., & Maupoey, P. F. (2018). An integrated approach for pineapple waste valorisation. Bioethanol production and bromelain extraction from pineapple residues. *Journal of Cleaner Production, 172*, 1224-1231. https://doi.org/10.1016/j.jclepro.2017.10.284

Gil, M. J., Soto, A. M., Usma, J. I., & Gutiérrez, O. D. (2012). Contaminantes emergentes en aguas, efectos y posibles tratamientos. *Producción+ limpia, 7*(2), 52-73.

González-García, P. (2018). Activated carbon from lignocellulosics precursors: A review of the synthesis methods, characterization techniques and applications. *Renewable and Sustainable Energy Reviews, 82*, 1393-1414. https://doi.org/10.1016/j.rser.2017.04.117

Hernández-Chaverri, R. A., & Prado-Barragán, L. A. (2018). Impacto y oportunidades de biorrefinería de los desechos agrícolas del cultivo de piña (Ananas comosus) en Costa Rica. *UNED Research Journal, 10*, 455–468.

Hock, P. E., Zaini, M. A. A., & Abbas, M. (2018). Activated carbons by zinc chloride activation for dye removal—A commentary. *Acta chimica slovaca, 11*(2), 99-106. https://doi.org/10.2478/acs-2018-0015

Hoque, M. B., Hossain, M. S., Nahid, A. M., Bari, S., & Khan, R. A. (2018). Fabrication and Characterization of Pineapple Fiber-Reinforced Polypropylene Based Composites. *Nano Hybrids and Composites, 21*, 31–42. https://doi.org/10.4028/www.scientific.net/nhc.21.31

Ioannidou, O., & Zabaniotou, A. (2007). Agricultural residues as precursors for activated carbon production-A review. *Renewable and Sustainable Energy Reviews, 11*(9), 1966–2005. https://doi.org/10.1016/j.rser.2006.03.013

Jagtoyen, M., & Derbyshire, F. (1998). Activated carbons from yellow poplar and white oak by H3PO4 activation. *Carbon, 36*(7–8), 1085–1097. https://doi.org/10.1016/S0008-6223(98)00082-7

Joseph, C. G., Fazli, H., Zain, M., Siti, &, & Dek, F. (2006). Treatment of Landfill Leachate in Kayu Madang, Sabah: Textural and Physical Characterization (Part 1). *Malaysia Journal of Analytical Sciences, 10*(1), 1–6.

Liou, T. H. (2010). Development of mesoporous structure and high adsorption capacity of biomass-based activated carbon by phosphoric acid and zinc chloride activation. *Chemical Engineering Journal, 158*(2), 129–142. https://doi.org/10.1016/j.cej.2009.12.016

Macedo, J. S., Otubo, L., Ferreira, O. P., de Fátima Gimenez, I., Mazali, I. O., & Barreto, L. S. (2008). Biomorphic activated porous carbons with complex microstructures from lignocellulosic residues. *Microporous and Mesoporous Materials, 107*(3), 276-285. https://doi.org/10.1016/j.micromeso.2007.03.020

Mahamad, M. N., Zaini, M. A. A., & Zakaria, Z. A. (2015). Preparation and characterization of activated carbon from pineapple waste biomass for dye removal. *International Biodeterioration and Biodegradation, 102*, 274–280. https://doi.org/10.1016/j.ibiod.2015.03.009

Maldonado, S. L. (2008). Estudio de la remoción de detergentes aniónicos tipo sulfato con carbón activado. *Escuela Politécnica Nacional*.

Marchena M., A. (2019). *Producción biotecnológica de biodiésel a partir de rastrojo de piña.*

Marsh, H., & Rodríguez-Reinoso, F. (2006). Activation processes (chemical). *Activated carbon*, 322-365. https://doi.org/10.1016/b978-008044463-5/50020-0

MINAE. (2007). *Reglamento de Vertido y Reuso de Aguas Residuales.*

Ministerio Comercio Exterior de Costa Rica. (2020). *Análisis sobre la evolución del comercio exterior e IED en Costa Rica: en 2019.*

Molina-Sabio, M., & Rodríguez-Reinoso, F. (2004). Role of chemical activation in the development of carbon porosity. Colloids and Surfaces A: *Physicochemical and Engineering Aspects, 241*(1–3), 15–25. https://doi.org/10.1016/j.colsurfa.2004.04.007

Nicolaas, E. S., Vega-Baudrit, J. R., Rodríguez, E., & Quesada, L. C. M. (2019). Estudio del efecto de la adición de nanocelulosa obtenida del desecho del rastrojo de piña en mezclas para materiales de construcción. *Revista Iberoamericana de Polímeros, 20*(1), 21-43.

Ortega, G. C. C., Viloria, C. A., Morrinson, C. A., Angulo, E. R., & Zambrano, A. M. (2017). Evaluación de un carbón activado comercial en la remoción del colorante DB2. *Revista Colombiana de Ciencia Animal-RECIA, 9*(2), 164-170. https://doi.org/10.24188/recia.v9.n2.2017.512

Olorundare, O. F., Msagati, T. A. M., Krause, R. W. M., Okonkwo, J. O., & Mamba, B. B. (2014). Activated carbon from lignocellulosic waste residues: effect of activating agent on porosity characteristics and use as adsorbents for organic species. *Water, Air, & Soil Pollution, 225*(3), 1-14. https://doi.org/10.1007/s11270-014-1876-2

Pezoti Junior, O., Cazetta, A. L., Gomes, R. C., Barizão, É. O., Souza, I. P. A. F., Martins, A. C., Asefa, T., & Almeida, V. C. (2014). Synthesis of $ZnCl_2$-activated carbon from macadamia nut endocarp (Macadamia integrifolia) by microwave-assisted pyrolysis: Optimization using RSM and methylene blue adsorption. *Journal of Analytical and Applied Pyrolysis, 105*, 166–176. https://doi.org/10.1016/j.jaap.2013.10.015

Quesada-Solís, K., Alvarado-Aguilar, P., Sibaja -Ballestero, R., & Vega-Baudrit, J. (2005). Utilización de las fibras del rastrojo de piña (Ananas comusus, variedad champaka) como material de refuerzo en resinas de poliéster. *Revista Iberoamericana de Polímeros, 6*(2), 157–179.

Rincón, N., Ramirez, W. M., Mojica, L. C., Blanco, D. A., Giraldo, L., & Moreno, J. C. (2014). Obtaining of activated carbon from seeds of eucalyptus by chemical activation with H_3PO_4. Characterization and evaluation of adsorption capacity of phenol from aqueous solution. *Ingeniería y Competitividad, 16*(1), 207–219.

Rincon, N. G., Moreno-Pirajan, J. C., & Giraldo, L. (2015). Preparación de carbón activado a partir de semilla de Eucalipto para la adsorción de compuestos fenólicos monosustituidos. *Afinidad, 72*(572).

Rincón, N. (2016). Obtención de carbón activado a partir de diferentes precursores lignocelulósicos: caracterización y evaluación de la capacidad de adsorción de contaminantes fenólicos. *Ingenium, 10*(27), 19–28.

Ravichandran, P., Sugumaran, P., Seshadri, S., & Basta, A. H. (2018). Optimizing the route for production of activated carbon from Casuarina equisetifolia fruit waste. *Royal Society Open Science, 5*(7). https://doi.org/10.1098/rsos.171578

Sann, E., & Adeeyo, S. (2016). Comparative analysis of adsorption of methylene blue dye using carbon from palmkernel shell activated by different activating agents. *University Convenant*, 175–181.

Sluiter, A., Hames, B., Hyman, D., Payne, C., Ruiz, R., Scarlata, C., ... & Wolfe, J. (2008). Determination of total solids in biomass and total dissolved solids in liquid process samples. *National Renewable Energy Laboratory, 9*, 1-6.

Solórzano, J. A., Gilles, J., Bravo, O., Vargas, C., Gomez-Bonilla, Y., Bingham, G. V., Taylor, D. B., & Rodriguez-Saona, C. (2015). Biology and trapping of Stable Flies (Diptera: Muscidae) developing in pineapple residues (Ananas comosus) in Costa Rica. *Journal of Insect Science, 15*(1), 145. https://doi.org/10.1093/jisesa/iev127

Tang, J., Zhu, W., Kookana, R., & Katayama, A. (2013). Characteristics of biochar and its application in remediation of contaminated soil. *Journal of Bioscience and Bioengineering, 116*(6), 653–659. https://doi.org/10.1016/j.jbiosc.2013.05.035

Thommes, M., Kaneko, K., Neimark, A. V., Olivier, J. P., Rodriguez-Reinoso, F., Rouquerol, J., & Sing, K. S. W. (2015). Physisorption of gases, with special reference to the evaluation of surface area and pore size distribution (IUPAC Technical Report). *Pure and Applied Chemistry, 87*(9–10), 1051–1069. https://doi.org/10.1515/pac-2014-1117

Tropea, A., Wilson, D., Torre, L. G. La, Curto, R. B. Lo, Saugman, P., Troy-Davies, P., Dugo, G., & Waldron, K. W. (2014). Bioethanol Production From Pineapple Wastes. *Journal of Food Research, 3*(4), 60. https://doi.org/10.5539/jfr.v3n4p60

Barrantes, É. V., & Alfaro, A. M. (2016). Costa Rica demanda una gestión integral del recurso hídrico: Escenario latinoamericano y la realidad país. *InterSedes, 17*(35). https://doi.org/10.15517/ISUCR.V17I35.25565

Wiel-Shafran, A., Ronen, Z., Weisbrod, N., Adar, E., & Gross, A. (2006). Potential changes in soil properties following irrigation with surfactant-rich greywater. *Ecological Engineering, 26*(4), 348–354. https://doi.org/10.1016/j.ecoleng.2005.12.008

Xu, F., Yu, J., Tesso, T., Dowell, F., & Wang, D. (2013). Qualitative and quantitative analysis of lignocellulosic biomass using infrared techniques: A mini-review. *Applied Energy, 104*, 801–809. https://doi.org/10.1016/j.apenergy.2012.12.019

Yahya, M. A., Al-Qodah, Z., & Ngah, C. W. Z. (2015). Agricultural bio-waste materials as potential sustainable precursors used for activated carbon production: A review. *Renewable and Sustainable Energy Reviews, 46*, 218–235. https://doi.org/10.1016/j.rser.2015.02.051

Yu, X., Zhang, K., Tian, N., Qin, A., Liao, L., Du, R., & Wei, C. (2015). Biomass carbon derived from sisal fiber as anode material for lithium-ion batteries. *Materials Letters, 142*(12), 193–196. https://doi.org/10.1016/j.matlet.2014.11.160

Zbair, M., Anfar, Z., Khallok, H., Ahsaine, H. A., Ezahri, M., & Elalem, N. (2018). Adsorption kinetics and surface modeling of aqueous methylene blue onto activated carbonaceous wood sawdust. *Fullerenes Nanotubes and Carbon Nanostructures, 26*(7), 433–442. https://doi.org/10.1080/1536383X.2018.1447564

Zubir, M. H. M., & Zaini, M. A. A. (2020). Twigs-derived activated carbons via H3PO4/ZnCl2 composite activation for methylene blue and congo red dyes removal. *Scientific Reports, 10*(1), 1–17. https://doi.org/10.1038/s41598-020-71034-6